REPRINTED FROM

Second Symposium on

NAVAL HYDRODYNAMICS

HYDRODYNAMIC NOISE

CAVITY FLOW

Sponsored by the

OFFICE OF NAVAL RESEARCH

and the

NATIONAL ACADEMY OF SCIENCES—
NATIONAL RESEARCH COUNCIL

August 25–29, 1958

Washington, D.C.

ACR–38

OFFICE OF NAVAL RESEARCH—DEPARTMENT OF THE NAVY

Washington, D.C.

AN EXPERIMENTAL STUDY OF CAVITATING INDUCERS

A. J. Acosta

California Institute of Technology

INTRODUCTION

The user of a turbomachine is mainly interested only in the overall hydrodynamic performance of the device. However, the designer is almost always confronted with the problem of achieving the intended performance in the face of many conflicting hydrodynamic and system requirements. In certain areas it may happen that a formerly deleterious effect (such as the occurrence of cavitation) can be turned to good advantage as in the case of the supercavitating hydrofoil or propeller. Unfortunately, this happy circumstance is not the lot of the designer of a liquid pumping system when the effects of cavitation are predominant. That this is so, follows from the fact that the dissipation effects in production of lift by a hydrofoil are relatively unimportant whereas dissipation is important in the decrease of energy of a fluid stream as in the case of a pump.

The basic compromise in pump design that makes cavitation a problem is rotative speed. If the size and weight of a pumping unit were immaterial, then a suitable combination of rotative speed and pump(s) could always be found to eliminate virtually any problem of cavitation. Fortunately for the occupational outlook of hydraulic engineers, one rarely has such freedom. In fact, weight and overall size are of such importance in missile turbopump applications that the conventional limits of rotative speed and cavitation criteria have been far exceeded, so that the effect of cavitation on overall performance is critical. A substantial reduction in weight is obtained, of course, by operation at high speeds, since to a rough approximation the tip speed for a given pressure rise is fixed. As the rotative speed is increased, the diameter is reduced and the weight is reduced more or less as the cube of the diameter. Needless to say, the weight of auxiliary driving equipment will also be smaller at high rotative speeds since, as is invariably the case, a high-speed impulse drive turbine is used and fewer gears will be needed in the reduction train. The flow near the inlet portions of the pump is now quite susceptible to cavitation because of the large relative velocities that occur in this region. Thus there is every incentive to operate a liquid pump at the highest possible rotative speed, limited only by cavitation.

These flows as well as non-rotating flows are governed by a cavitation index k except that herein they are based upon the inlet relative velocity dynamic pressure, the upstream static pressure and the vapor pressure of the flowing fluid. Some appreciation of the fluid dynamic effects to be expected may be gained by a comparison of the cavitation numbers at which conventional pumps operate and those of modern

propellant pumps. A well-designed centrifugal (or axial) pump may be expected to operate with cavitation numbers as low as about 0.3 before serious deterioration in performance occurs. However, a missile propellant pump may be called upon to operate satisfactorily with values of $k = 0.03$, say, although at some loss of efficiency. (To make the comparison fair, the service life of the conventional unit as determined by cavitation damage will be many times that of the propellant pump.) It is clear that with such low values of k, a cavitation-free flow cannot be obtained and, in fact, considerations of cavitation dominate the design of inlet portions of such machines.

A characteristic feature of cavity flows in confined spaces is that for a given geometry there is a minimum cavitation number below which steady flow is not possible. This effect may be termed "choking" in analogy with the compressible phenomenon or cavitation "breakdown." Examples of such limiting flows in ducts are given in Ref. 1 and in cascades in Ref. 2. In the case of a pump operating at a given speed and flow rate, there also exists an inlet pressure below which maintenance of the flow rate is not possible. It is extremely important in design to be able to predict the minimum required inlet pressure, and to so design the machinery as to make this minimum as small as the circumstances allow.

From the foregoing remarks it will have been anticipated that the inlet configuration of a pump designed for cavitation will be quite different from a conventional machine. At small cavitation numbers (say less than 0.1) the cavity length becomes appreciable, and for the limiting cavitation number, the cavity length is infinite—at least in all planar flows. It is no surprise, then, that the blade length of the inlet portions of pumps for cavitating service must be long, or at least sufficiently long to insure finite cavity lengths over the desired operating range. The length of the blade is conveniently expressed in units of the circumferential blade spacing, and the ratio of these lengths is called the solidity. The inlet portions of such pumps will therefore be of high solidity (at least greater than unity) and to avoid high local velocities will be predominantly axial. For convenience of manufacture, this inlet region is often made separately and subsequently joined to the main stage. Following supercharger terminology, this separate piece is called an "inducer." The function of the inducer is to pressurize the flow sufficiently to enable the following pumping equipment to perform satisfactorily. If the primary rotor is of the centrifugal type, the pressure increase of the inducer portion usually needs to be only about ten percent of the pressure rise of the system. The power requirement of the inducer is then not an overriding consideration and the necessary cavitation performance of this component can then be obtained at the cost of efficiency if need be.

The inducer is thus only an extension of the main rotor. Its being separate, however, offers advantages in that it may be run at a different speed on a coaxial shaft and certain fabrication difficulties are alleviated. Figure 1 is a photograph of a typical pump-inducer combination.* The inducer is hardly a new device. For example, one of the very first rocket engines, the Walter 109-509A engine for the Me-163 rocket plane, used an inducer-pump combination (3). In the intervening period there has been a rapid development of inducers and pumps for cavitating service by organizations interested in missile development. However, relatively little design information has appeared in the open literature. We find, for example, Zimmerman in 1950 discussing the effect of pump suction pressure requirements in terms of pumping machinery weight (4). Brumfield (5) and Ross (6) undertook an elementary analysis to show in effect that there is an optimum inlet diameter for a

*For a novel scheme to eliminate the inducer, and for a good discussion of the problem, see Wislicenus, G.F., "Critical Considerations on Cavitation Limits of Centrifugal and Axial-Flow Pumps," Trans. ASME 78:1707 (1956).

given speed and flow rate. Ross was particularly interested in demonstrating the effect of inlet conditions on weight and Brumfield pointed out the advantages of pre-whirl in attaining low inlet pressures. The first paper dealing explicitly with the inducer was by Ross and Banerian (7) in which the function of the inducer is outlined and a general description of the flow is given. They report few details about the internal flow in the inducer but show that extremely low inlet pressures can be achieved.

Fig. 1 - A typical inducer installation on a centrifugal pump for liquid oxygen. (Courtesy of Mr. T. Carter, Turbocraft Corp., Pasadena.)

Both the photograph of Fig. 1 and those in Ref. 7 show the inducer to be generally helical in shape. It is usually machined, and in these examples consists of a helical surface, the lead of which may vary from inlet to discharge. The hub diameter as well as the tip diameter may also vary along the axis. Although there are many design variables, the general appearance of an inducer is a rotor of high solidity, small number of blades, and small blade angle. The purpose of this paper is to report the results of some experiments on typical inducer shapes. These experiments are intended to show in a qualitative way the general flow patterns in the inducer in various stages of cavitation from incipient to near breakdown. For this objective the simplest (but still useful) inducer shape is chosen; a rigid helix of constant lead. Three blade tip angles were studied, namely, 6°, 9°, and 12°. The solidity was kept constant at 2.5 for each of these investigations. Additional tests were made with the 9° impeller by varying the solidity from 1.0 to 3.25 and by changing the tip clearance over a wide range.

Complete performance data (cavitating and noncavitating) was obtained for each of the foregoing arrangements. As will be seen, the flow through such a simple geometrical device is extremely complicated and not subject to exact analysis (although this may not be necessary for design). In the following sections the noncavitating and cavitating performance of these inducers will be presented, together with some simple correlations based on two-dimensional free streamline theory. It will be shown that while we are not able to predict well the occurrence of breakdown the correlations found do offer "rules of thumb" for design that will serve until better information becomes available.

EXPERIMENTAL PROGRAM

The Test Rotors

The combination of flow coefficients and head coefficients required for inducer applications lies far outside conventional pump or fan practice. Accordingly, it was desired to cover a reasonably wide range of geometric variables in the test program. To simplify construction not only of the rotor but the rotor housing, the blade shapes (as noted before) were rigid, helical surfaces with tip blade angles of 6°, 9°, and 12°. The tip diameter was 2 inches and the hub diameter was 1 inch. The solidity for the 6° and 12° rotors was maintained at 2.5 whereas it was systematically varied in the

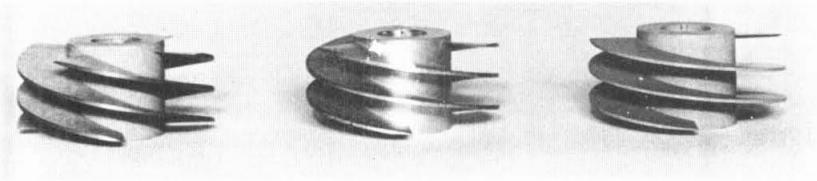

Fig. 2 - The 6°, 9°, and 12° experimental inducers. The tip diameter is 2 inches.

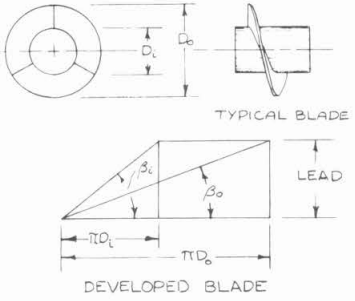

Fig. 3 - Definition sketch of impeller geometry

9° series from unity to 3.25. The tip clearance was also systematically varied in the 9° series for a given solidity (2.5) over a wide range.

Figure 2 is a photograph of several of the rotors tested. The various configurations tested are tabulated in Table 1, and Fig. 3 may be consulted for the definitions of the various geometrical terms.

All impellers were machined from 25 ST aluminum stock and anodized for corrosion and damage protection. The blade thickness was about 0.045 inch at the tip for most of the impellers. The leading edges in all cases were sharpened so that the resulting shape was a wedge with about a ten-degree included angle.

Test Facility

At the start of this program no suitable test facility was available. The design of the arrangement shown in Fig. 4 was determined by the available funds and the desire for a simple, reliable, and compact system. The hydraulic circuit consists of a 60-gallon storage tank on which are mounted the cylindrical Lucite working section (Fig. 4) and the drive motor and associated controls. Considerations of the available motors and power supply dictated that the diameter of the working section be 2 inches. For maximum visual observation of the flow, the impellers were mounted on a 1-inch shaft that is supported by a water-lubricated bearing upstream and a grease-lubricated ball bearing in the downstream diffusor. A mechanical face-seal prevents water from getting into the bearing or prevents air from leaking into the circuit when operating at low pressures. A three-legged spider (with struts of 9-percent thickness) supports the upstream bearing. The support is 1-1/2 diameters upstream of the impeller so that no appreciable wake effects should remain in the flow.

The discharge from the diffusor then passes through a turbine-type flowmeter and an auxiliary circulating pump. The hydraulic circuit is completed by discharge back into the 60-gallon reservoir. The ambient pressure in the circuit is changed by applying vacuum or pressure to a separate container about 1 gallon in volume that is in turn connected to the storage tank. This tank is mounted approximately 1 foot above the working section, and purge lines from all high points in the circuit lead to it so that undissolved air obtained either by deaeration of the water or during the normal course of operation at low pressure can be removed.

Table 1

Constants of Impellers Tested
Nominal Tip Diameter = 2.0 in.; Hub Diameter = 1.000 in.

Impeller No.	Blade Tip Angle (deg)	Solidity	No. of Blades	Radial Tip Clearance (in.)	Tip Clearance Ratio (gap/blade height)
1	12.05	2.5	4	0.002	0.004
2	12.05	2.5	4	0.005	0.010
3	9.1	2.5	3	0.0015	0.003
4	9.1	2.5	3	0.004	0.008
5	9.1	2.5	3	0.008	0.016
6	9.1	2.5	3	0.020	0.040
7	9.1	2.5	3	0.0055*	0.011
8	9.1	3.25	3	0.0055	0.011
9	9.1	2.0	3	0.0055	0.011
10	9.1	1.5	3	0.0055	0.011
11	9.1	1.0	3	0.0055	0.011
12	6.1	2.5	2	0.0045	0.009

*This impeller appears to have systematic manufacturing differences between it and the preceding ones of the same blade angle.

The greatest compromise in the design of the test system was the impeller drive motor. With the small diameter (2 inches) of the rotor it is necessary to operate at high rotative speeds to obtain the low cavitation numbers sought. (Since hydraulic horsepower varies as the cube of the speed, and fifth power of the diameter, a small rotor operating at high speed is demanded if the power required is not to be excessive for a given tip speed.) The minimum useful rotative speed for cavitation studies was thought to be about 9000 rpm. A survey of the electric motor market quickly showed that no induction motor suitable for the laboratory variable frequency supply was readily available, and as a compromise choice a 1/2-hp universal motor was obtained that could operate at rotative speeds from 6000 to 12,000 rpm. The motor power output was calibrated at several speeds, and electrical input power measurements were subsequently used to establish the pump efficiency. This procedure was not completely satisfactory since the motor calibration depended upon the operating temperature as well as load.

Instrumentation

All pressures were measured with mercury manometers. The flow rate was found from the rotative speed of a calibrated turbine-type flowmeter. Although the

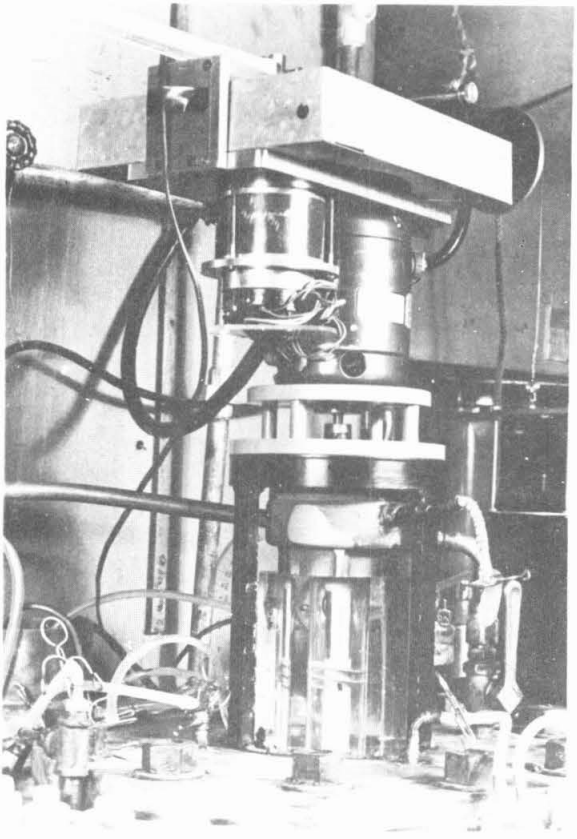

Fig. 4 - View of test facility showing the Lucite working section and the drive motor. The discharge piping and manometers are not visible.

motor speed was manually varied and controlled, it was measured by comparing it with the output of a known speed source. The comparison speed was capable of being varied in discrete units of 12 rpm. In practice, the armature current was varied until there was no difference between the motor speed and that of the source. The details of this system can be found in Ref. 8.

The impeller total head was measured with a small impact probe 0.05 inch in diameter at a station 1.5 inches downstream from the impeller. Surveys near the hub or case were made with a boundary layer probe 0.02 inch in height. Flow angles and static pressures were also measured in the midstream portion of the annulus. However, owing to the relatively large size of these instruments and the high curvature of the flow in the passage, accurate measurements of these quantities could not be obtained near the walls.

Procedure

The limitation to the relatively low tip speeds of the present tests (about 90 ft/sec) required the inlet static pressures to the impeller be on the order of 5 feet absolute. The first step therefore in the tests was to deaerate the water to levels such that the fluid was not supersaturated with air at these inlet pressures. For all except the very lowest inlet pressures this was achieved by limiting the air content to 3 ppm (i.e., moles of air per mole of water). A Van Slyke blood gas analyzer was used to measure the air content. Needless to say, much time was expended in obtaining and maintaining the air-tightness of the system to get such relatively low values of dissolved air. Even so, an air content of say 1/2 ppm would have been preferable.

In these experiments the performance of the machine is separated into cavitating and noncavitating performance. The latter tests were made to get a general idea of the flow within the impeller and to see how the performance of such machines compared with that of more conventional designs. For this purpose, total head, flow rate, and input power measurements were made. Extraneous torques such as seal friction were measured by the electric power input to the motor and computations of the efficiency could then be made.

The cavitation tests were made by maintaining constant flow rate and speed and decreasing the system ambient pressure. The ambient pressure was lowered until the impeller could not maintain the given flow rate (termed cavitation breakdown) or the system minimum inlet pressure was reached. Operation near the breakdown point was quite unstable, since the power requirement of the impeller varied widely and constant speed could not be obtained with a universal motor. For this reason data at breakdown itself is of limited extent and most of the deductions made were based on information obtained near this point.

The quantity of principal interest in the cavitating tests was the total-pressure rise. It was measured at the downstream station in the middle of the annulus (at a radius ratio of 0.75). Although the total head at this position corresponds to a rough average of the total head over the annulus, the head so measured must be smaller than the properly weighted total head. The results thus obtained are conservative.

Both cavitating and noncavitating performance data were taken for each of the impeller combinations listed in Table 1. Studies on somewhat modified impeller forms were also made but will not be reported here. In fact, because of the large amount of experimental data gathered, only those salient features of impeller performance both cavitating and noncavitating will be mentioned.

RESULTS

To facilitate the presentation, the noncavitating features of the flow through the inducers will be discussed first. As a further aid in visualizing the flow, the results of a tuft study made on a 12° inducer (No. 1, Table 1) will be given.

Tuft Photographs (Noncavitating)

Figure 5 shows a sequence of three photographs of a 12°-impeller operating various flow-rate coefficients. As seen in this picture, three rows of three tufts each are fastened to the case and in addition three tufts are mounted on the hub immediately upstream and downstream of the rotor. At the highest flow rate shown ($\phi = 0.10$, occurring at about the maximum efficiency), the upstream tufts show little

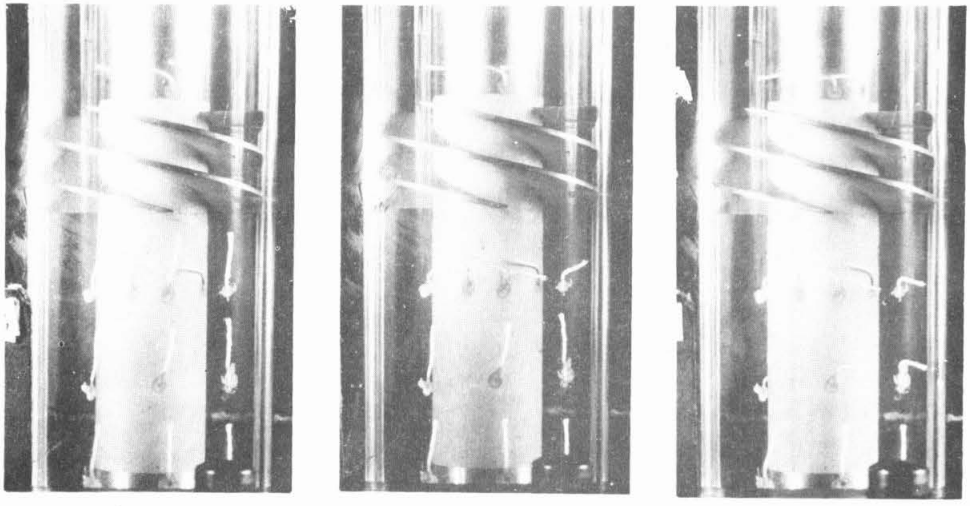

$\varphi = 0.10$ $\varphi = 0.08$ $\varphi = 0.06$

Fig. 5 - Sequence of tuft photographs on a 12° impeller at various flow rates. The rotation is from left to right and flow approaches the rotor from below.

or no disturbance and the hub tufts are in accordance with a smooth relative flow there. At the intermediate flow rate ($\varphi = 0.08$), however, the row of tufts nearest the impeller on the case show a strong influence from the impeller whereas the hub tufts are still relatively unaffected. At $\varphi = 0.06$ back flows on the case upstream of the impeller and on the hub immediately downstream of the trailing edge are quite noticeable.

Thus at the lowest flow rate shown any resemblance to straight axial flow is gone. The general circulation pattern in the meridian plane appears to be that of the strong ring vortices discussed by Spannhake (9). Additional visual tuft studies were made on a 9° impeller to confirm this point. From these it appears that at flow coefficients for which the strong upstream flow disturbance is observed, the suction surface of the blade near the leading edge is not separated. However, tufts on the pressure surface at the outside diameter indicate that a strong tip clearance flow at the leading edge may be the agent of the disturbance. The tip clearance in these observations was 1 percent of the blade height, but more observations with variable tip clearance are necessary before this question can be settled.

The course of the flow through the rest of the impeller is fairly complicated at these flow rates. Strong radial inflow on the pressure side of the blade just downstream of the leading edge was observed on the inner half of the blade height and secondary flows were observed on the hub. About halfway through the impeller, the flow on the hub appears to separate. The back flow at the trailing edge on the hub shown in Fig. 5 flows into this region. A compensating radial outflow is observed on the pressure side of the blade near the trailing edge.

Although the flow patterns just described ($\varphi = 0.08$ on the 12° inducer and 0.075 on the 9° impeller) are not yet fully understood, it seems certain that the upstream

disturbance is not a result of blade stall and centrifugal pumping action. It may be therefore that the resemblance between the present flow and that described by Spannhake is purely coincidental.

Overall Performance (Noncavitating)

Pump performance is usually expressed in terms of a dimensionless head coefficient ψ and flow coefficient ϕ (see Notation). The noncavitating performance of impellers 2, 3, and 12 is given in Fig. 6. (Recall that the total head was measured at the midpassage position.) The efficiency even under noncavitating conditions is rather low (about 75 percent), by ordinary standards. The excessive passage length, poor flow conditions at the leading edge, and tip clearance leakage all contribute to this low figure.

Several elementary estimates of the pressure rise curve were made, none of which were wholly successful. One of these is shown in Fig. 6 for the 9° impeller. It was obtained by assuming that the root-mean-square radius was typical for the machine, by assuming that there is perfect guidance of the flow by the blades, by accounting for blockage due to vane thickness, and by subtracting off a "friction" loss based on an equivalent number of passage diameters and the relative velocity. At the best efficiency point this estimate is 22 percent high. It would be surprising if such a simple procedure were to work well, since it is known that a helical surface cannot impart a constant total head to all radii and since it is apparent that strong real fluid and tip clearance effects occur. Figure 7 shows a flow survey taken 1.5 diameters downstream of impeller 7 at a flow coefficient of $\phi = 0.093$ (near the best efficiency point). The local flow coefficient and total head coefficient vary appreciably but smoothly across the channel. The velocity profile and output

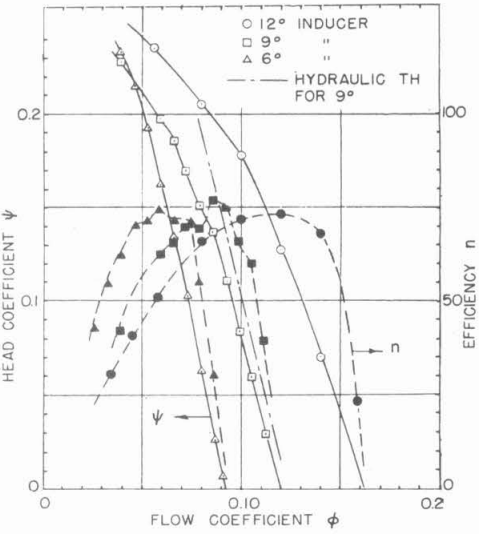

Fig. 6 - Noncavitating efficiency and head coefficient vs flow coefficient for a 6°, 9°, and 12° helical inducer (impellers 12, 3, and 2) and solidity of 2.5

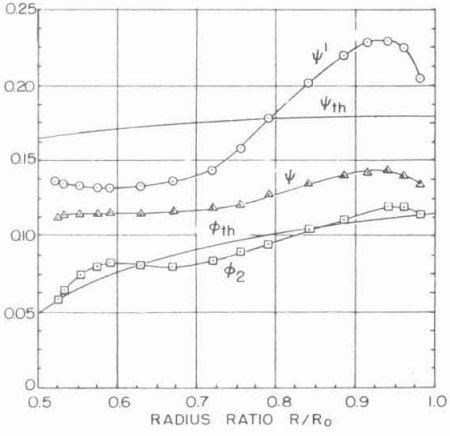

Fig. 7 - Measured axial velocity profile ϕ_2, measured head coefficient ψ, measured input head coefficient ψ', theoretical axial velocity, and theoretical head coefficient distributions across the annulus of a 9° helical inducer at a mean flow coefficient of $\phi = 0.093$

total head coefficient were computed on the basis of the simple radial equilibrium theory of Ref. 10 and are also shown on Fig. 7. (In these calculations, a constant 12-percent blockage of the annulus due to vane thickness was assumed.) The observed axial velocity profile follows the theoretical trend adequately but there is a great departure of the observed ψ' curve from the radial equilibrium value. We are not able to explain fully the reasons for the wide discrepancy except to remark that tip clearance leakage and the three-dimensional flows that undoubtedly take place violate the assumptions of perfect guidance and lossless relative flow used in the radial equilibrium computations. These effects are so pronounced at a flow coefficient only 7 percent lower (i.e., $\varphi = 0.087$) that the axial velocity profile is nearly linear and is zero at the hub. At lower flow coefficients reverse flow is measured at the hub verifying the type of flow pattern shown in Fig. 5. For these conditions the simple radial equilibrium theory fails.

The flow-rate coefficient computed from the downstream velocity survey agreed satisfactorily with the measured value for a flow coefficient of 0.093 and higher. As a check on the electrical measurement of power input to the impeller, the torque was computed from the angular momentum measurements of Fig. 7. The agreement between these two methods was excellent (within 5 percent). In common with other investigations (11), an increase in tip clearance is found to decrease the maximum efficiency of the impellers, to reduce the head coefficient, and to increase the torque required. Over the range of tip clearances shown in Table 1, the maximum efficiency is reduced by 25 percentage points, and the head is reduced by 20 percent. Somewhat surprising is the finding that the head coefficient is nearly a linear function of the solidity at a given flow rate. For example (see Fig. 17), when the solidity is increased from unity to 3.25 the head coefficient at a flow coefficient of $\varphi = 0.093$ increases from 0.083 to 0.12 or an increase of about 45 percent. A detailed explanation of this phenomenon must await further experiment since according to two-dimensional unseparated cascade flow theory, substantially all of the guiding effect of a flat plate blade row is achieved when the solidity is about unity.

Performance During Cavitation

It is convenient when making cavitation tests to maintain the flow geometry and hence the flow coefficient constant and observe the change in head as a function of a cavitation parameter. In the pump and turbine literature the customary cavitation index is the "suction specific speed," a quantity closely related to the more familiar cavitation number, which may be converted into the suction specific speed (S) by means of the formula in the Notation section. The total-head output of impellers 2, 3, 12 as a function of cavitation number was determined as discussed above and is shown in Fig. 8. A common feature of all of these curves is that the head is essentially unaffected until the cavitation number is 0.1 or less. Even then, the head drops off only slowly (except for the low flow rates) until a cavitation number is reached at which a further decrease causes the very rapid decrease in performance known as cavitation breakdown. As mentioned previously, limitations of the circuit prevented obtaining breakdown for all conditions. However, some definite breakdown points are shown in Fig. 8 and even for those flow rates when no sharp decrease occurs, at the minimum value of k shown, breakdown is imminent.

These diagrams show that extremely low cavitation numbers can be achieved (in the order of 0.03) for all impellers, so that suction specific speeds in the range 25,000 to 30,000 can be readily achieved (although at the risk of cavitation damage). However, these plots do not reveal the interesting and complicated flow patterns that develop as cavitation takes place. To illustrate these points, a number of photographs of the 12° impeller will be used. The first series (Fig. 9) shows the impeller

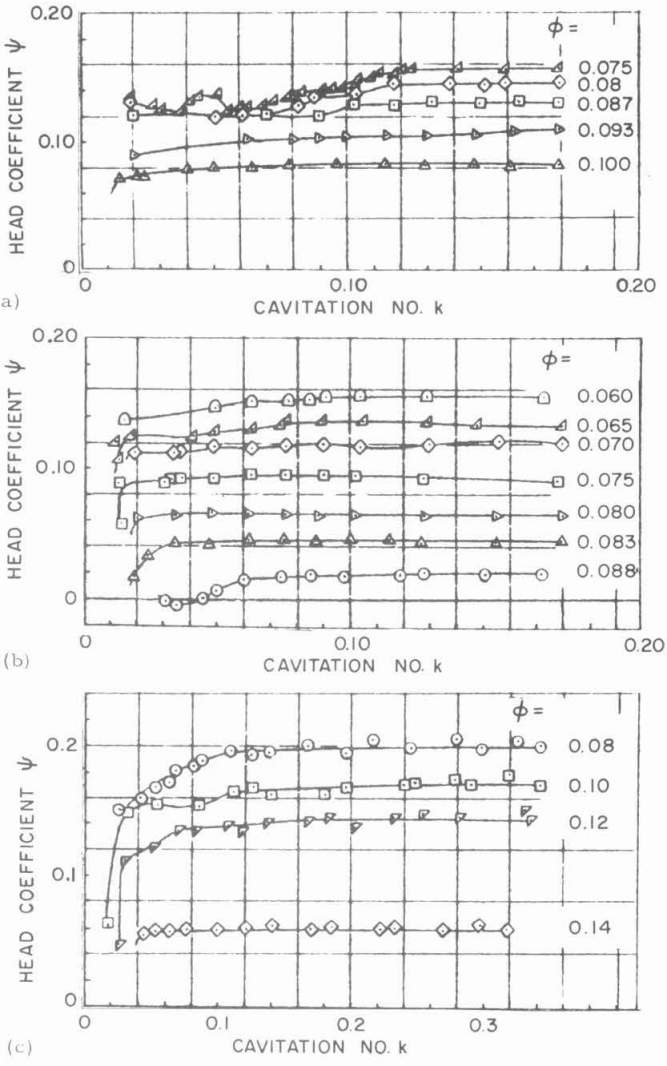

Fig. 8 - Cavitation performance of a series of helical inducers of 2.5 solidity and 0.5 hub ratio; (a) 12° inducer (impeller 2), (b) 9° inducer (impeller 3), (c) 6° inducer (impeller 12)

operating at a flow coefficient in the good efficiency range ($\varphi = 0.12$) as the inlet pressure or cavitation number is lowered. A patch of cavitation is seen at the blade tip in Fig. 9 that grows as the pressure is lowered until at $k = 0.02$ it is about 3/4 as long as the blade. The cavitation bubble is never clear, as it is on a sharp-edge hydrofoil in a water tunnel, but always has a frosty appearance. Close inspection shows that the greatest part of the fuzzy cavitation patch arises from a tip clearance flow similar to that reported in Ref. 12. The cavitation is confined largely to the outer portions of the annulus, but at the lowest cavitation numbers it does occur from root to tip. The development shown in Fig. 9 satisfies one's intuitive idea of the growth of cavitation but at other flow coefficients the sequence is entirely different as for example those in Figs. 10, 11, and 12. In Fig. 10 ($\varphi = 0.14$) we see every other blade cavitating. This arrangement is stable and it does not always occur on the same blades. At lower flow rates, the alternate blade cavitation appears to propagate from blade to blade in much the same way as propagating stall in a cascade. The frequency of propagation depends upon the cavitation number, being high at high k's

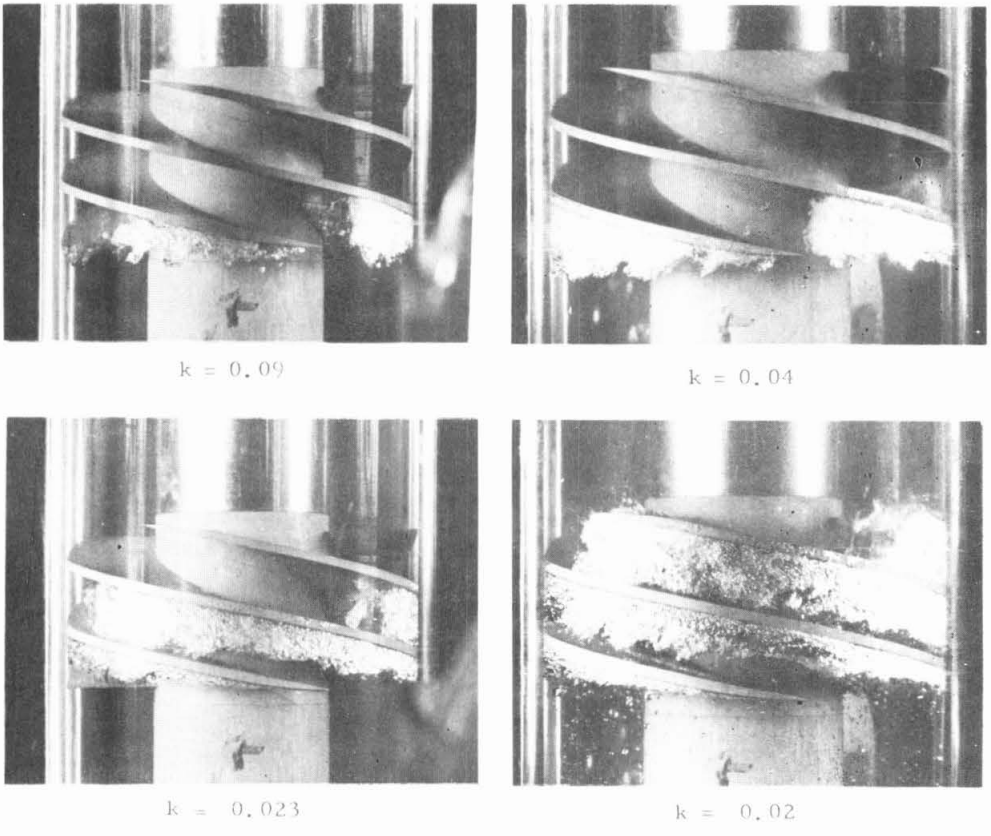

Fig. 9 - Development of cavitation in a 12° helical inducer for a flow rate coefficient $\varphi = 0.12$. (These photographs are not strictly in a sequence since they were taken at different times and rotative speeds.)

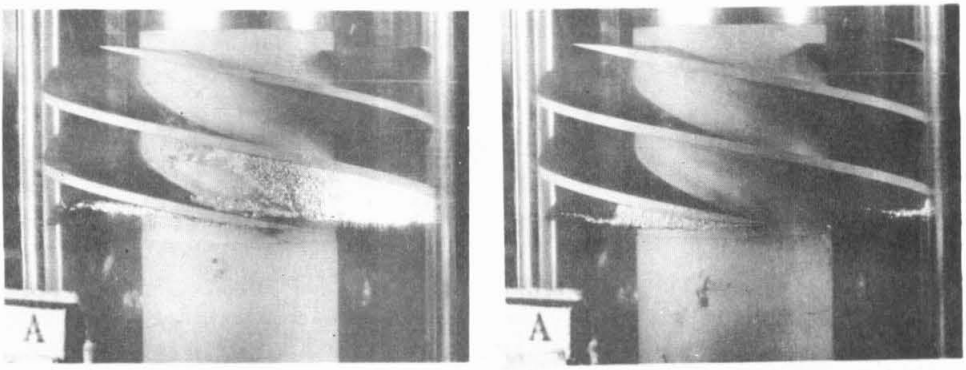

k = 0.06 k = 0.16

Fig. 10 - Cavitation on the 12° inducer at a flow coefficient of $\varphi = 0.14$, showing the occurrence of alternate blade cavitation

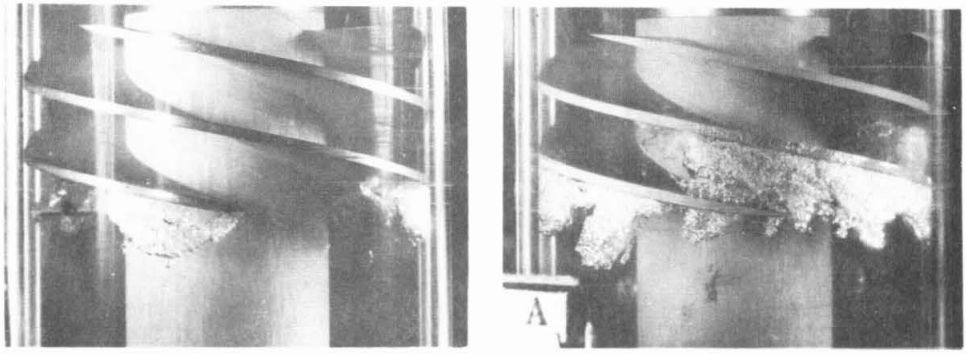

k = 0.22 k = 0.056

Fig. 11 - Cavitation on the 12° inducer at a flow coefficient of $\varphi = 0.10$. The confused flow pattern at the lower cavitation number is typical of nonsteady oscillating cavitation.

and decreasing to zero frequency just before cavitation breakdown.* In this regime blade forces can be quite high and the various mechanical parts of the pump assembly can be easily excited to resonance. It is difficult to show the state of the flow in this "oscillating cavitation" condition but Fig. 11 gives some idea of the disturbed flow present. At even lower flow rates the back-flow phenomena illustrated in Fig. 5 gives rise to a spectacular vortical flow (Fig. 12). Even this peculiar flow pattern is able to achieve very low cavitation numbers (shown at breakdown in the last of this sequence).

*The occurrence of these phenomena had been pointed out to the author by Dr. Toru Iura in 1955.

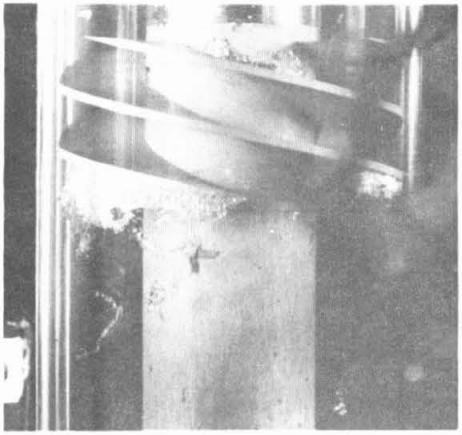

k = 0.15

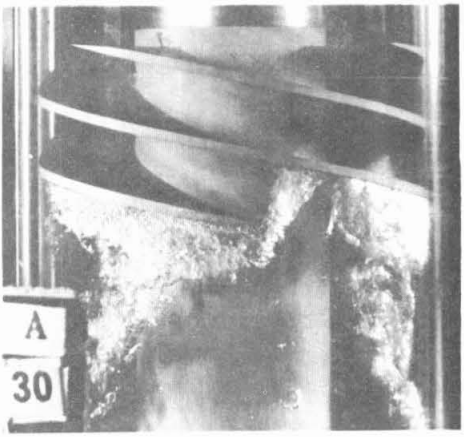

k = 0.13

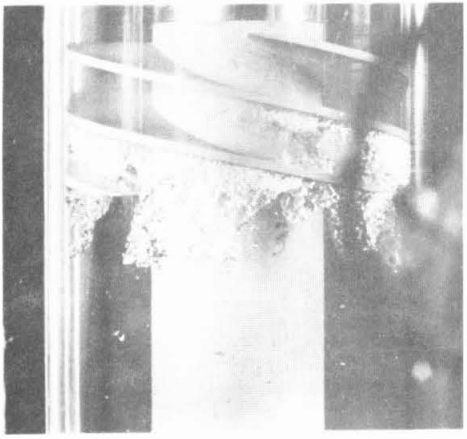

k = 0.07

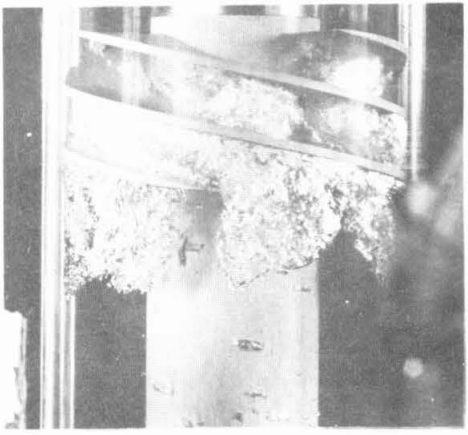

k = 0.03

Fig. 12 - Cavitation development at a flow coefficient of $\phi = 0.08$ on the 12° inducer

A diagram showing the location of these various regions is shown in Fig. 13. The boundaries of these regions are not sharply defined and depend to a considerable extent on the details of the leading edge design and somewhat on the tip clearance. However, it is typical of all of the helical inducers studied. The outlines of the oscillating cavitation region are also shown in Figs. 8b and 8c for the other blade angles.

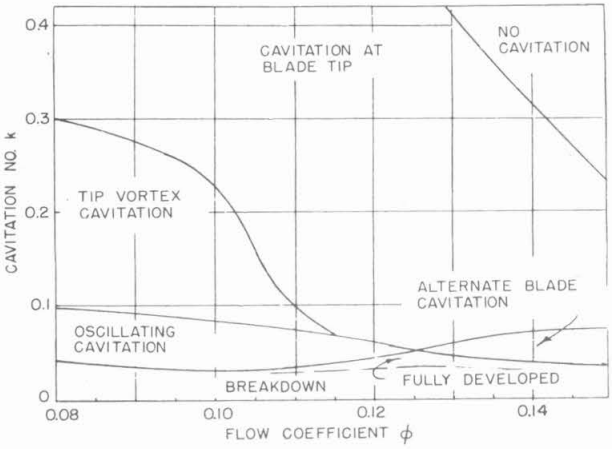

Fig. 13 - The various modes of cavitating flow in a 12° helical inducer as a function of cavitation number and flow coefficient

From these diagrams we see that most applications for highly cavitating inducers will be subject to this phenomenon, and accordingly some effort was made to find simple modifications of the impeller that would suppress it. Three were tried: (a) increasing the tip clearance, (b) changing the leading edge contour of the impeller and (c) varying the lead of the impeller blades from inlet to discharge. Increasing the tip clearance offered some help (in preventing oscillating cavitation) but at the expense of cavitating performance and overall efficiency. No extensive leading edge modifications were carried out, but the one tried which consisted of making the leading edge of the blade surface a spiral rather than a radial line, depressed the occurrence of oscillating cavitation to lower cavitation numbers and also improved the cavitation performance! In the last attempt an impeller was constructed with a blade angle of 6° at the inlet and 9° at the discharge and with a solidity of 2.5. The overall performance was similar to the 9° impeller and the cavitation performance was similar to the 6° impellers (although not quite as good), but the extent and severity of the oscillating mode was greatly reduced. The foregoing remarks imply that this zone is to be avoided at all cost. This is believed to be the case only for mechanical reasons, since there is no hydraulic reason to do so.

It has already been mentioned that increased tip clearance tends to reduce hydraulic performance. The same result is also found to be true when cavitation occurs, as Fig. 14 shows. According to the present results the smallest possible tip clearance gives the best cavitation performance. Even so, impressively low k's are still achieved with the largest clearance used, although at greatly reduced output. (It should be mentioned here that there is probably no particular merit in making the tip clearance dimensionless with the blade thickness since for the ranges of Reynolds number used inertial forces prevail in the gap, and the rotor radius is then a better characteristic length (11).) Photographs taken of cavitation with the largest tip clearance suggest that the increased tip clearance flow that takes place gives rise to large disturbances in the outer portions of the passage that cavitate prematurely and thereby lower the output head.

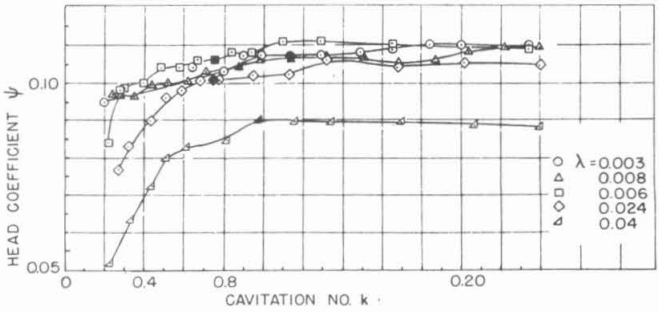

Fig. 14 - The effect of tip clearance on the cavitating performance of a 9° inducer with a solidity of 2.5 at a flow coefficient near the best efficiency point (φ = 0.093). The solid symbols indicate inception of oscillating cavitation.

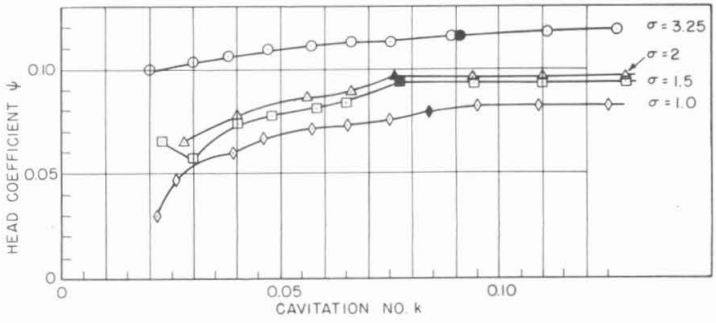

Fig. 15 - The effect of solidity on the cavitating performance of a 9° helical inducer at a flow coefficient of φ = 0.093. The solid symbols denote inception of oscillating cavitation.

The effect of solidity on cavitation performance is shown in Fig. 15. It is somewhat surprising that extremely low cavitation numbers can be achieved with a solidity as low as unity. However, the head had dropped off by a factor of three at the minimum k of 0.02 for σ = 1, whereas for σ = 3.25, the head had only decreased by 20 percent at the same k.

Some velocity profile measurements were also obtained during cavitating flow for a 9° impeller (No. 7) to see if significant changes occurred in the distributions of Fig. 7. Interestingly enough it was found that cavitation improved the axial velocity profile. The distribution of total head across the passage remained about the same although, of course, lower. At flow coefficients ranging over the efficiency peak of this impeller, and at all cavitation numbers, cavitation decreased the torque of the impeller as found from the velocity surveys. The efficiency, however, still decreased with decreasing k.

DISCUSSION

Cavitation Breakdown

One of the intentions of this work was to correlate the breakdown cavitation number with the impeller geometry. From the foregoing remarks it is seen that while there are examples of clearcut cavitation breakdown, both the limitation of the equipment and phenomenon itself do not always allow such a black-and-white distinction to be made. Nevertheless, many points at cavitation numbers below which operation was not practical were observed—both visually and with measurements. In all of the cases where breakdown had either occurred or was imminent, the length of the cavitation region was between 75 and 100 percent of the blade chord. In no case did the cavitation region extend beyond the chord before breakdown had occurred. The reason for this is quite clear since before breakdown the increase in the total head (and hence static pressure) is of the order of 10-15 p :cent of the tip velocity head. This pressure is much higher than the inlet pressure and is responsible for collapsing the cavity. But for this pressure rise and hence total pressure rise to exist, a peripheral velocity ΔW_u of about 10-15 percent of the tip speed must be imparted to the flow. From Fig. 16 it is seen that a whirl velocity of this magnitude cannot be obtained with a high solidity cascade of flat plates if the leaving relative velocity is comparable to the velocity on a cavity boundary (i.e., greater than the inlet velocity).

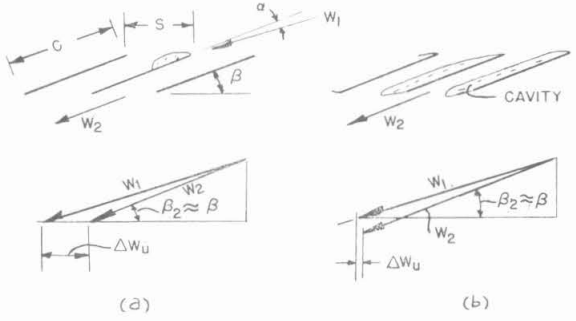

Fig. 16 - Velocity triangles in a flat plate cascade
(a) without and (b) with extensive cavitation

The question then arises as to whether we can make a reasonable estimate of the cavitation number when the cavitating region is nearly as long as the chord. We will certainly have to exclude flow-rate coefficients less than the maximum efficiency point to rule out the strong three-dimensional effects seen in Fig. 12. For similar reasons impellers with large tip clearance will have to be excluded. Even then from the analysis of noncavitating results (Fig. 7), the main flow through the impeller is not frictionless nor wholly two-dimensional. Even so, correlations based on theory would be useful to have, even if they are ultimately empirical. For this purpose it was assumed that the flow through the helical impeller was equivalent to the flow through a two-dimensional cascade of flat plates with a streamline springing free at the leading edge and forming a partial cavity of length less than the chord. Now it is known that the linearized free streamline theory does not provide a solution to the problem of the partial cavity on an isolated plate when the cavity length in a reasonable fraction of the chord (12). Consequently, the view was taken that as far as the growth of the cavity in an inducer of high solidity is concerned, the most

significant length is the circumferential spacing between the blades. The length of the blades was then taken as infinite compared with the spacing and the growth of a partial cavity in such a cascade was carried out by exact and linearized free streamline methods.

The results of both methods agreed well except for large cavitation numbers where the limitations of the linearized theory were exceeded. Values of cavity length vs cavitation number were also calculated (by the linearized theory) for a cascade geometry equivalent to the mean radius of the 9° impeller at a flow coefficient of $\varphi = 0.093$, and the results of this calculation are shown in Fig. 17. Also plotted in Fig. 17 are approximate lengths of the cavity as determined by visual measurements. The agreement is hardly overwhelming but several points are worth mentioning: (a) the general trend of both curves is the same although a systematic difference for small lengths and high k's is found; (b) the minimum cavitation number is reached very soon after the ratio of cavity length to spacing is 1-1/2, thereby indicating that excessively high solidities are unnecessary; and finally (c) our empirical observation is that for practically all the flow rates and impellers tested (6°, 9°, and 12°) the minimum cavitation number reached before breakdown was less than two times the minimum cavitation number possible in a given cascade with a given angle of attack. In the present example the minimum is the asymptote of the curve shown in Fig. 17. The value of this asymptote can be obtained quite simply from elementary momentum considerations when it is recalled that there is no net force parallel to the plate and that the cascade is sufficiently long so that the flow is perfectly guided (see also Ref. 13). The result of this calculation is that the minimum cavitation number achievable in a cascade of infinitely long flat plates is $k \approx \alpha(\beta - \alpha)$ where α and β are the local angle of attack and blade angle respectively (both of these values to be small). This relation has a maximum of $\beta^2/4$ and is zero at $\alpha = 0$ and $\alpha = \beta$. The first

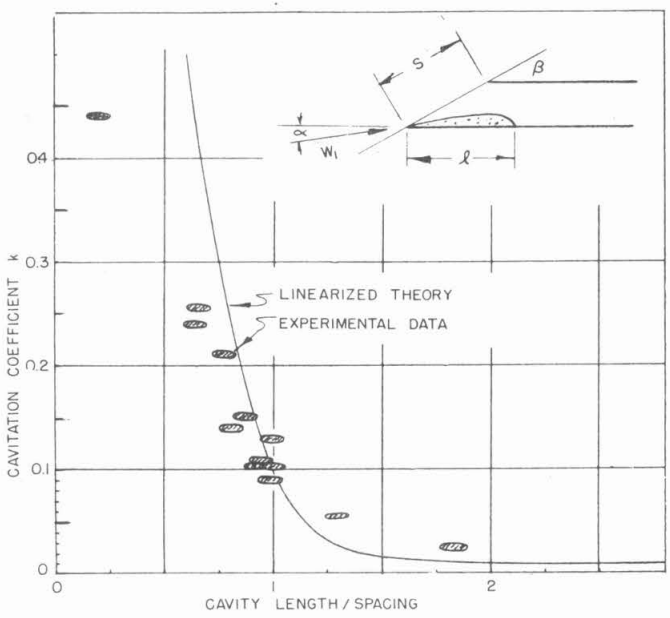

Fig. 17 - Growth of a partial cavity in a cascade as a function of cavitation number. The angle of attack and blade angle correspond to the mean radius of the 90° impeller at a flow coefficient of $\varphi = 0.093$.

result follows from the assumed zero thickness of the blades, and the latter, although perhaps surprising, only occurs when there is zero flow through the blade row. This formula also shows that smaller blade angles are better for obtaining lower cavitation numbers and this conclusion is qualitatively borne out by the present experiments.

The present calculations, although crude, account for the trends in breakdown occurrence, at least for sufficiently high solidities and flow rates where the flow is predominantly two dimensional. Further work along these lines employing more elaborate models will be reported in the future.

Cavitation Similitude

In the absence of friction or body forces the cavitation number determines the location and extent of cavitation on a body. The only question is, What is the pressure in the cavity? In the present experiments the cavity pressure was assumed to be the vapor pressure of the bulk fluid, since it was not possible to measure it directly. This assumption cannot be right since in a fluid containing dissolved air, the cavity pressure can exceed the vapor pressure by the amount of the air diffused into the cavity. This possibility was investigated by removing the impeller and blocking the annulus of the test section to a sufficient extent to create a cavity behind a small lamina. The pressure in the cavity was found to be 20 to 25 percent higher than the vapor pressure of the fluid, (the air content in the water was the same as that in the inducer tests) confirming similar experiments of Parkin and Kermeen (13). We suspect therefore that the cavitation numbers listed in the present report are too high, but in lieu of direct measurement we have preferred to base them on the equilibrium vapor pressure of the liquid. Of course in pure liquids with no dissolved air (e.g., liquid oxygen) the pressure may be less than the vapor pressure of the bulk fluid due to thermal effects in evaporating the liquid to fill the cavity. It is known, for example, that cavitation performance in liquid oxygen is better than that in tap-water and it is almost certainly for this reason. At present several groups are working on this problem but no conclusive results are available yet.

Further Remarks

There are a number of difficult problems that remain to be solved before the understanding of cavitating flows in rotating machines is well in hand. They are, in fact, nearly too numerous to mention, for in addition to embracing the unknowns of the turbomachine field, the many effects of cavitation are included. Nevertheless, with the aid of a few rules of thumb and some empirical data such as that presented herein, an inducer can be designed for a specific application with a minimum of development. Thus even with our imperfect understanding of the cavitating flow through machines, the pumping of liquids at extremely low ambient pressures offers no insuperable problems.

ACKNOWLEDGMENT

A great part of the experimental work was done by Lt. H. J. Nawoj, U.S.N., and Capt. S. H. Carpenter, U.S.M.C. The author would like to acknowledge his debt to them and to the skillful talents of Mr. J. R. Kingan. This work was supported by the Office of Naval Research.

NOTATION

c = chord

h = head (ft of water)

k = cavitation number = $(p_1 - p_k)/(\rho W_1^2/2)$

N = rpm

p = pressure

r = radius

s = spacing between blades

S = suction specific speed =

$$\frac{N\sqrt{gpm}}{(h_{t1} - h_v)^{3/4}} = 8140\ \varphi^{1/2} \left(1 - \frac{r_i^2}{r_o^2}\right)^{1/2} \Bigg/ \left[(1 + \varphi)^2 k + \varphi^2\right]^{3/4},$$

where gpm is the flow rate in gallons per minute

U = tip speed $(r\omega)$

V = absolute velocity

W = relative velocity

α = angle between blade chord and inlet relative velocity

β = blade angle measured from plane of rotation

η = efficiency

λ = ratio of tip clearance to blade height

ρ = density

σ = solidity = c/s

φ = flow coefficient = average axial velocity $/U_o$ except as noted

ψ = measured total head coefficient = gh_t/U_o^2

ψ' = input head coefficient = $r(V_{u2} - V_{u1})/r_o U_o$

ω = angular speed

Subscripts

1 = far upstream	k = cavity
2 = far downstream	t = total quantity
i = hub	u = component parallel to tip speed
0 = case	v = denotes vapor

REFERENCES

1. Birkhoff, G., Plesset M., and Simmons, N., "Wall Effects in Cavity Flow-I," Quart. App. Math. 8:151 (1950)

2. Betz, A., and Petersohn, E., "Anwendung der Theorie der frien Strahlen," Ingenieur Archiv, Band II (1931)

3. Sutton, G.P., "Rocket Propulsion Elements," 2nd ed., New York:Wiley, 1956, p. 252

4. Zimmerman, J.E., "Effect of Pump Performance on Liquid Propellant Rocket Design," American Rocket Society, preprint No. 79-52 (1952)

5. Brumfield, R.C., "A Study of Pump Rotor Blade Cavitation Parameters," U.S. Naval Ordnance Test Station, TM 549, 1951

6. Ross, C.C., "Principals of Rocket Turbopump Design," J. Rocket Soc., March 1951

7. Ross, C.C., and Banerian, G., "Some Aspects of High-Suction-Specific-Speed Pump Inducers," Trans. ASME 78:1715 (1956)

8. Knapp, R.T., Levy, J., O'Neill, J.P., and Brown, F.B., "The Hydrodynamics Laboratory of The California Institute of Technology," Trans. ASME 70:437 (1948)

9. Spannhake, W., "Centrifugal Pumps, Turbines and Propellers," Cambridge:M.I.T. Technology Press, 1934

10. Bowen, J.T., Sabersky, R.H., and Rannie, W.D., "Theoretical and Experimental Investigations of Axial Flow Compressors," California Institute of Technology, Eng. Div. Report, 1949

11. Rains, D.A., "Tip Clearance Flows in Axial Flow Compressors and Pumps," California Institute of Technology, Eng. Div. Report No. 5, 1954

12. Acosta, A.J., "A Note on Partial Cavitation of Flat Plate Hydrofoils," California Institute of Technology, Hydrodynamics Laboratory Report No. E-19.9, 1955

13. Parkin, B., and Kermeen, R.W., "Water Tunnel Techniques for Force Measurements on Cavitating Hydrofoils," J. Ship Research 1(No. 1):36 (1957)

* * * * *

A. J. Acosta

DISCUSSION

T. Iura (Space Technology Laboratory)

I wish to supplement Dr. Acosta's results with some data obtained three years ago in the inducer test facility at Rocketdyne.

The cavitation patterns observed with helical inducers were similar to those described by Dr. Acosta. For inducers with four blades, at a given flow coefficient, a reduction in cavitation number produced the following sequence of cavitation behavior:

1. Initial cavitation - equal on all blades at the blade tips
2. Alternate blade cavitation - stable patterns on alternate blades
3. Oscillating or propagating cavitation
4. Fully developed cavitation - equal on all blades.

Figure D1, a cavitation performance curve of a 16.2-degree helical inducer, illustrates the cavitation regimes mentioned. The alternate blade and unstable cavitation patterns were most pronounced at the flow rates below the maximum-efficiency point while stable alternate blade cavitation pattern was not observed on inducers with an odd number of blades; asymmetric unstable patterns were in evidence between the initial and fully developed invitation regimes. The oscillating cavitation consisted

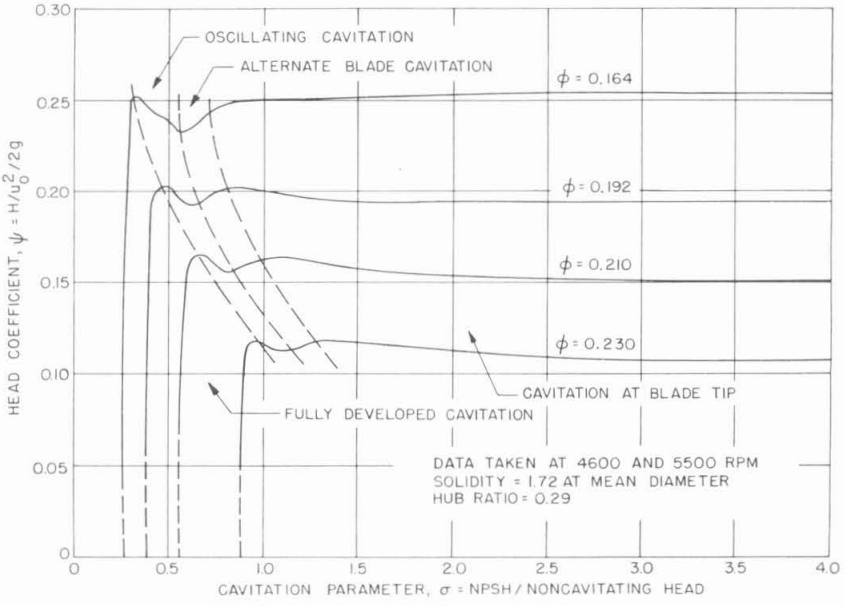

Fig. D1 - Cavitation performance of 16.2-degree (at tip) four-bladed helical inducer

of the cavitation pattern oscillating along the blade length in a highly erratic manner. In one case (for a 11.2-degree helical inducer) a definite propagation pattern was observed. The propagation speed, based on observations of high speed movies, was about one-tenth of the inducer rotative speed.

In regard to vibration accompanying inducer cavitation, Fig. D2 gives a qualitative picture of the vibration levels obtained with a 14.6-degree helical inducer. The measurements were made with a vibration pickup mounted on the test section. As the cavitation number (or net positive section head) is lowered, the vibration increases steadily through the first three zones of cavitation. The maximum vibration level occurs just prior to fully developed cavitation after which it decreases rapidly due to bubbles collapsing in midstream rather than against the blade surfaces.

In Fig. D3, the dimensionless breakdown NPSH (net positive suction head) is plotted as a function of the mean-diameter helix angle for various angles of attack. The breakdown NPSH is defined here as that value of NPSH at which the inducer head has completely dropped to zero. These data were obtained from tests of seven inducers ranging in tip solidity from 1.07 to 2.44. It was found that the breakdown NPSH was rather insensitive to solidity, although the rate of head drop-off was quite sensitive to solidity as pointed out by Dr. Acosta. Along with the breakdown NPSH data, the theoretical calculations based on Betz-Petersohn's two-dimensional analysis are plotted. The theoretical breakdown curve has the same slope as the experimental data, but falls considerable below the actual results. Although the trend of breakdown is indicated by the two-dimensional model, there certainly is a need for the more elaborate models mentioned by Dr. Acosta and for a three-dimensional model.

Figure D4 shows the maximum inducer efficiency as a function of solidity, and Fig. D5 shows the cavitation parameter corresponding to the maximum-efficiency points plotted as a function of solidity.

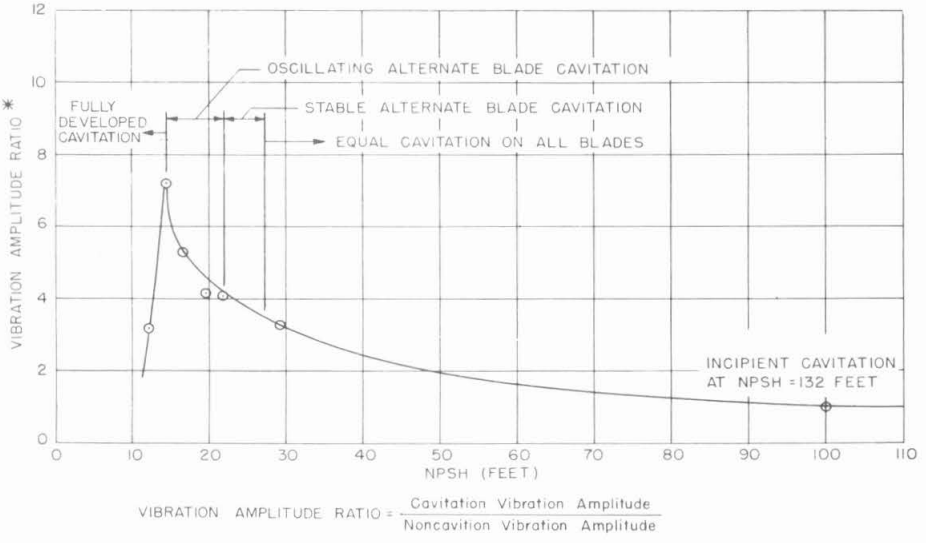

Fig. D2 - Cavitation vibration data of 14.6-degree helical inducer (amplitude measurements with vibration pickup on test section)

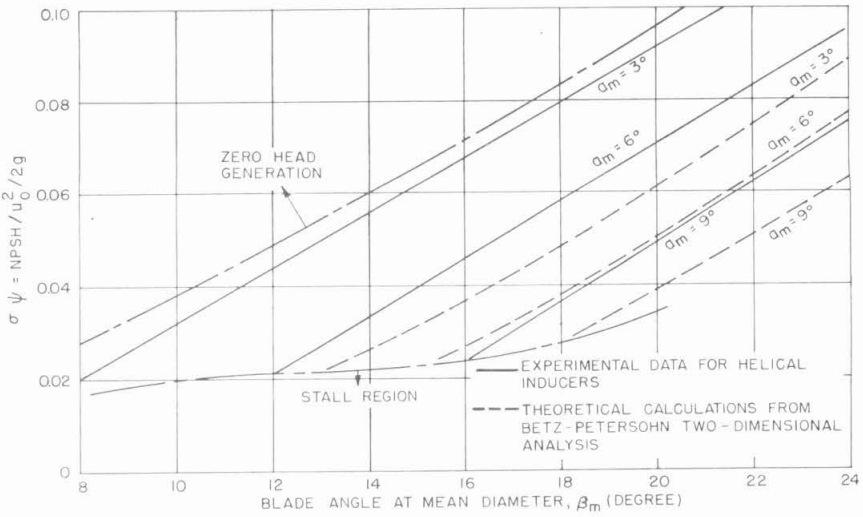

Fig. D3 - Cavitation head-breakdown characteristics of helical inducers comparison of theory and experimental results

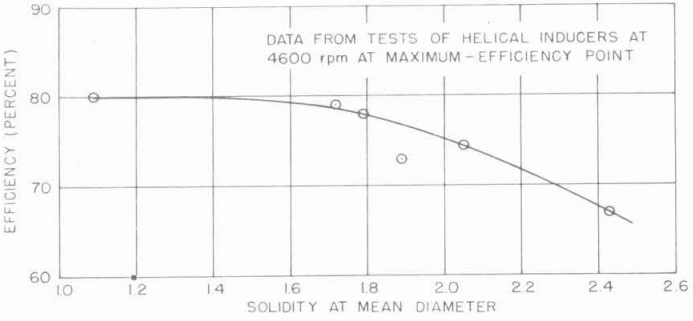

Fig. D4 - Effect of solidity on inducer efficiency

In regards to cavitation similitude, tests at Rocketdyne on centrifugal pumps with inducers show that cavitation performance in liquid oxygen is better than that in water, and in liquid nitrogen is better than that in liquid oxygen. For a given type of pump, the critical NPSH (one percent head drop-off point) in water was 1.3 times that in liquid oxygen and 1.9 times that in liquid nitrogen. However, these values are dependent on inlet conditions such as flow rate and design blade angle. With the inducer taken out of the same centrifugal pump, tests between water and liquid oxygen no longer showed a consistent difference in cavitation performance.

If one calculates the comparative vapor-bubble growth rates from Plesset and Zwick's theory (for superheated liquid), it is found that water has 10 times the growth

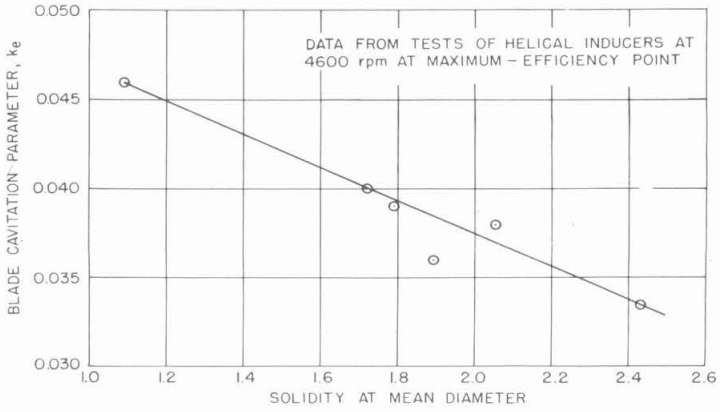

Fig. D5 - Effect of solidity on blade cavitation parameter

rate of liquid oxygen or liquid nitrogen. However, Plesset's theory does not show much difference between the growth rate of liquid oxygen and liquid nitrogen. Clearly, some theory is needed to correlate the thermodynamic properties of the liquid with the dynamic features of the pump flow in order to explain the different behavior in various fluids.

A. J. Acosta

It is clear that many organizations, such as Rocketdyne and Aerojet-General Corporation, have been actively working in this field for some time to good effect. I regret that they have not previously found opportunity to present their results. To some degree perhaps, the present paper may assist in bringing their work out.

It is gratifying that many of the observations made by Dr. Iura, evidently on larger experimental apparatus, verified in a general way our findings at the California Institute of Technology.

* * * * *